

# Systematic Errors in Emission Cross Sections Arising in the Analysis of Laboratory Beam Measurements

H. A. B. Gardiner, John J. Merrill, W. R. Pendleton, Jr., and Doran J. Baker

A technique for obtaining emission cross sections in laboratory beam studies is presented, including effects on the cross section due to polarization of the emitted light. Systematic analytical errors arising from optical problems are analyzed and evaluated for a typical spectral feature. The primary sources of error are shown to arise from the particular geometry used in the optical measurements, the variation of the calibrating light source over the bandwidth of the emission feature, and the variation of the responsivity of the optical system over the bandwidth.

## Introduction

In laboratory beam experiments for studying collision-induced radiation, an absolute emission cross section  $\sigma_{jk}(v)$  is commonly defined as the mean number of quanta of wavelength  $\lambda_{jk}$  which are emitted per unit length of path as a result of collisional interactions between a single beam particle and a gas of unit number density. (The relative velocity of the beam and target particles prior to the collision is designated by  $v$ .)

The definition suggests three optical problems that arise in the experimental determination of absolute emission cross sections: (1) a determination of the angular distribution of the radiation emitted by collisionally excited atoms or molecules, (2) a determination of the volume from whence the observed emission emanates, and (3) a calibration of the absolute responsivity of the optical system used to measure the irradiance of the beam. If any of these problems are inadequately considered, serious errors in the emission cross section data can result.

A treatment of systematic errors associated with these problems in emission cross section measurements seems particularly timely, inasmuch as differences in calibration procedures are thought to be mainly responsible for a factor-of-two discrepancy that currently persists between the emission cross section data reported by various investigators.<sup>1-11</sup> The situation is illustrated by the presently available data for the excitation of the (0, 0)  $N_2^+$  first negative band ( $\lambda 3914 \text{ \AA}$ ) as a result of proton or electron impact.

Although within regions of overlapping projectile energy the energy dependence of the cross sections for a particular projectile is found to be approximately the same, the data reported by one group of investigators<sup>1-5</sup> are scaled roughly a factor of two higher than the data reported by another group.<sup>6-10</sup> This disparity is somewhat greater than the uncertainty in the cross section measurements (typically less than  $\pm 40\%$ ). Similar discrepancies exist in the literature for other projectile-target systems.

## Objectives and Approach

The objectives of this paper are to outline a practical technique for obtaining absolute emission cross sections in laboratory beam experiments and to evaluate the magnitude of possible systematic uncertainties inherent in the use of this method. The concern here is only with those uncertainties which arise from optical problems. Thus, this paper does not treat such problems as beam current and target gas pressure measurement, projectile energy, etc., which in their own right may contribute significantly to the total uncertainty of the emission cross sections.

The approach of this paper is to deduce first the angular distribution of the light from the beam by the polarization of the light. The light is treated analytically as arising from dipole oscillators. A computation of the total integrated response of the detection system to a general spectral feature is then made, in which changes of the responsivity with wavelength and polarization are taken into account. The above response is then compared with that which results from viewing a blackbody reference source instead of the beam. An absolute calibration is achieved by taking into account the actual emission volume under observation in each case.

The result is given as a formula for the emission cross section. In this formula, aside from the expected

---

H. A. B. Gardiner is with the Radiation Effects Branch, Optical Physics Laboratory, AFCRL, Bedford, Massachusetts 01730; the other authors are with the Electro-Dynamics Laboratories, Utah State University, Logan, Utah 84321.

Received 24 July 1968.

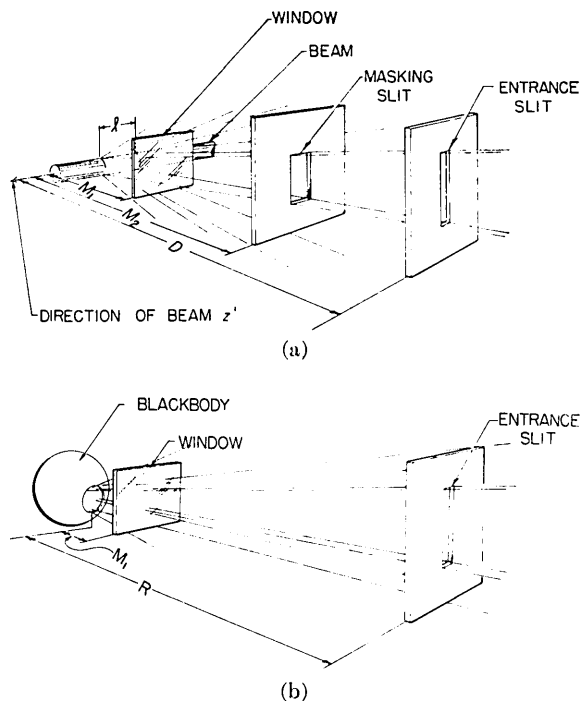


Fig. 1. (a) Schematic drawing illustrating the calibration geometry used in the beam experiment. (b) Schematic drawing illustrating the geometry used in illuminating the entrance slit of the spectrometer with radiation from the blackbody source.

Note: The drawings are not to scale.

factors, a correction term appears which provides a measure of the systematic analytical error that can arise in the determination of emission cross sections.

Although the experimental geometry and the calibration light source discussed in this paper differ in some important particulars from those used in earlier measurements of this kind, much of the following analysis is directly applicable to most such experiments. The remainder serves as an example of the type of analysis which must be accomplished for each experimental arrangement.

## The Experimental Technique

The geometry of our beam experiment for obtaining emission cross sections is shown in Fig. 1(a). An incident beam of fast-moving particles collides with a dilute gaseous target. Radiation emitted at nearly right angles to the direction of the beam passes out of the collision chamber through a window of high transmissivity and is accepted by the entrance slit of a scanning monochromator. This radiation is emitted from a small length of beam of volume  $V$ , with  $V$  approximately cylindrical in shape and sharply framed by a masking slit interposed between the beam and the entrance slit. The detector is a multiplier phototube mounted at the exit slit of the monochromator. The response of the monochromator-detector system for specific emissions from the beam is noted as a function of wavelength, target chamber pressure, beam current, etc. Owing to the low light intensity levels normally

encountered in such an experiment, special care is taken to prevent extraneous radiation from entering the detection system.

This geometry differs from that which has been used by most investigators in that there is no lens between the beam and the monochromator. In addition, the entrance slit of the monochromator is perpendicular, rather than parallel, to the beam direction. Both of these factors tend to simplify the calibration analysis. Furthermore, this geometry of the monochromator slit is essential if the experiment is to measure emissions that change significantly with position along the beam.

Representative values of the geometrical parameters that have been used in this laboratory for emission cross section measurements are given in Table I. Since, in this geometry, the separation  $D$  of the entrance slit from the ion beam is much greater than the diameter of the beam or the dimensions of the slit, the volume  $V$  appears in a first approximation as a point source emitter. The geometry has the advantage that departures from a point source, point detector geometry are made evident if calculations of radiative quantities are expressed in powers of  $D^{-1}$ .

The absolute responsivity of the optical system is found by observing its spectral response to a blackbody standard. The advantages of a blackbody as a calibrating light source are well known: The emission is reliably characterized by a single parameter, the temperature; and the absolute spectral radiance can be accurately calculated from Planck's law over a large spectral range. As with any calibrating source, some care must be exercised in using a blackbody source over an extended spectral interval owing to problems of overlapping orders and scattered light within the monochromator. These problems can usually be overcome by the use of appropriate spectral filters.

The geometry used in illuminating the entrance slit with light from the blackbody is shown in Fig. 1(b). A window identical to the one used in the beam experiment is interposed between the aperture of the black-

Table I. Geometrical Parameters of the Beam Experiment

	Symbol	Magnitude (cm)
1. Monochromator slit width	$a$	<0.05
2. Monochromator slit length	$b$	<2.50
3. Masking slit width	$a'$	0.51
4. Separation of window from center of beam	$M_1$	10.4
5. Separation of masking slit from center of beam	$M_2$	17.8
6. Maximum radius of beam	$r'_{\max}$	0.16
7. Length of beam observed	$l$	0.68
8. Separation of entrance slit from center of beam	$D$	68.6
9. Separation of entrance slit from blackbody aperture	$R$	56.0
10. Diameter of blackbody aperture	$b'$	0.25-1.52
11. Thickness of chamber window	$d$	0.64

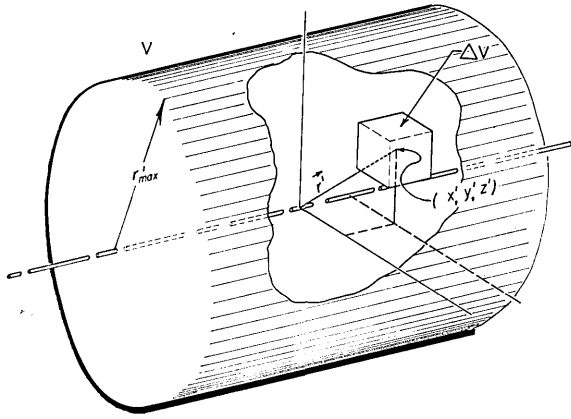


Fig. 2. Schematic illustration of the geometry used in treating the radiation from a collection of dipole oscillators.

body and the entrance slit to conveniently take into account transmission losses in the beam experiment. The separation of the entrance slit from the aperture, denoted by  $R$ , is much larger than the dimensions of either the aperture or the slit, and  $R$  is approximately the same as  $D$ . The size of the entrance slit is fixed throughout the entire experiment.

### Angular Distribution of the Radiation and the Polarization Fraction

Since it is impractical to measure directly the angular distribution of radiation from the beam, radiative anisotropy is deduced from polarization measurements with the aid of theory. In this procedure, the electric dipole radiation emitted from the beam is hypothesized to be produced by a set of radiating oscillators. The oscillators are assumed to be noninteracting, incoherent sources, and their emission is required to duplicate all of the macroscopic properties of the beam radiation including the polarization and spatial distribution.

The angular distribution of the radiation emitted by a single, nonrelativistic oscillator has the dependence  $|\hat{n} \times (\hat{n} \times \mathbf{p})|^2$ , where  $\hat{n}$  is a unit vector directed from the region of the oscillator to a distant point of observation, and  $\mathbf{p}$  is the polarization vector describing the orientation and dipole strength of the oscillator. The distribution of oscillators contained in an incremental volume  $\Delta V$  (see Fig. 2) located at a point  $(x', y', z')$  can be envisaged by referring all the polarization vectors associated with the oscillators to a common origin. The three-dimensional space into which the polarization vectors extend is conveniently described by spherical polar coordinates  $p$ ,  $\theta_p$ , and  $\phi_p$ , with the pole aligned parallel with the direction of the beam ( $z'$  axis). The number of polarization vectors which terminate in a volume  $\Delta^3 p = p^2 \sin \theta_p \Delta p \Delta \theta_p \Delta \phi_p$  yields the density of oscillators having dipole strength  $p$  and orientation described by the angles  $\theta_p$  and  $\phi_p$ .

The total number of photons of all polarizations that are emitted per unit time from  $V$  with wavelengths between  $\lambda$  and  $\lambda + \Delta\lambda$  and which are accepted by the

entrance slit of the monochromator can be expressed as

$$N(\Omega_s, \lambda) \Delta\lambda = t(\lambda) \int d^3 p \int_{\text{slit}} d\Omega \times \int_V d^3 r' \epsilon(\mathbf{r}', \mathbf{p}, \lambda) |\hat{n} \times (\hat{n} \times \mathbf{p})|^2 (\lambda/hc) \Delta\lambda, \quad (1)$$

where  $h$  is Planck's constant,  $c$  is the speed of light *in vacuo*, and  $t(\lambda)$  is the transmissivity of the collision chamber window at a wavelength  $\lambda$ . The distribution function  $\epsilon(\mathbf{r}', \mathbf{p}, \lambda)$  describes the number of oscillators in  $\Delta V$  which have polarization vectors in  $\Delta^3 p$  and emit photons having wavelengths in the spectral interval between  $\lambda$  and  $\lambda + \Delta\lambda$ . The unit vector  $\hat{n}$  is explicitly given by

$$\hat{n} = (\mathbf{r} - \mathbf{r}') / |\mathbf{r} - \mathbf{r}'|. \quad (2)$$

The total number of photons, described by Eq. (1), having electric field vectors parallel with a unit vector  $\hat{m}$  is found by replacing  $\hat{n} \times (\hat{n} \times \mathbf{p})$  by its projection along  $\hat{m}$ . This quantity will be denoted as  $N_m(\Omega_s, \lambda) \Delta\lambda$ .

The  $\phi_p$  integral in Eq. (1) can be evaluated if use is made of the symmetry properties of the beam. The symmetry principle invoked here is that the distribution function  $\epsilon(\mathbf{r}', \mathbf{p}, \lambda)$  is cylindrically symmetric about the  $p_z$  axis. Deviations from this symmetry in a laboratory situation arise primarily from two sources: (1) the presence within the collision chamber of electromagnetic fields which may tend to favor scattering in specific azimuthal directions about points within the beam, and (2) the acquisition by a beam particle of a velocity component transverse to the axis of the beam. Such a component can arise from the passage of a nearly monoenergetic beam through a magnetic field or from small angle collisional scattering of beam particles.

The effects of these symmetry destroying influences can be considerably reduced by shielding the target chamber from the terrestrial magnetic field and the fringe fields of the magnetic analyzer, by narrowly collimating the beam, and by restricting observations to sufficiently low target chamber pressures so that small angle scattering is minimal. If these precautions are taken, the assumption of azimuthal symmetry is valid, at least as a first approximation.

When the  $\phi_p$  integration in Eq. (1) is performed, the result is

$$N(\Omega_s, \lambda) \Delta\lambda = t(\lambda) \int_0^\infty dp \int_0^\pi d\theta_p \int_{\text{slit}} d\Omega \times \int_V d^3 r' (T + U \cos^2 \theta_p) g(\mathbf{r}', p, \theta_p, \lambda) (\lambda/hc) \Delta\lambda, \quad (3)$$

where

$$g(\mathbf{r}', p, \theta_p, \lambda) \equiv \pi p^4 \sin \theta_p \epsilon(\mathbf{r}', \mathbf{p}, \lambda)$$

with  $T \equiv 1 + n_z^2$  and  $U \equiv 1 - 3n_z^2$ . The expression for  $N_m(\Omega_s, \lambda) \Delta\lambda$  is also given by Eq. (3), with  $T$  and  $U$ , respectively, replaced by

$$T_m \equiv 1 - m_z^2 + 2m_z n_z (\hat{m} \cdot \hat{n}) - (1 + n_z^2) (\hat{m} \cdot \hat{n})^2, \\ U_m \equiv 3m_z^2 - 1 - 6m_z n_z (\hat{m} \cdot \hat{n}) + (3n_z^2 + 1) (\hat{m} \cdot \hat{n})^2. \quad (4)$$

At this point in the development, it is convenient to introduce the polarization fraction of the radiation, defined by

$$\Pi(\lambda) \equiv \lim_{D \rightarrow \infty} \frac{N_{||}(90^\circ, \lambda) \Delta\lambda - N_{\perp}(90^\circ, \lambda) \Delta\lambda}{N_{||}(90^\circ, \lambda) \Delta\lambda + N_{\perp}(90^\circ, \lambda) \Delta\lambda}, \quad (5)$$

where  $N_{||}(90^\circ, \lambda) \Delta\lambda$  and  $N_{\perp}(90^\circ, \lambda) \Delta\lambda$  are the rates at which photons of wavelength  $\lambda$  are emitted at an angle of  $90^\circ$  to the beam, having electric vectors parallel with or perpendicular to the direction of the beam, respectively. The limit  $D \rightarrow \infty$  enters Eq. (5) because the measured polarization, in general, depends on the source-detector distance.

The polarization fraction defined in Eq. (5) differs from the polarization fraction  $\Pi_e(\lambda)$  measured at a finite  $D$  by a small term  $\delta\Pi_e(\lambda)$ . The term  $\delta\Pi_e(\lambda)$  arises because the entrance slit accepts some radiation which is emitted at angles slightly different from  $90^\circ$  to the beam. Although the absolute value of  $\delta\Pi_e(\lambda)$  for the present geometry can be shown to be less than 0.01 (see Appendix II) for any positive value of  $\Pi(\lambda)$ , more serious uncertainties can arise if the magnitudes of  $r'_{\max}$ ,  $l$ ,  $a$ , and  $b$  relative to  $D$  are somewhat larger than in the geometry used here.

By the use of Eqs. (4) and (5), the polarization fraction can be written as

$$\Pi(\lambda) = (-1 + 3\theta)/(1 + \theta), \quad (6)$$

where

$$\theta \equiv \frac{\int_0^\infty dp \int_0^\pi d\theta_p \int_V d^3r' g(\mathbf{r}', p, \theta_p, \lambda) \cos^2\theta_p}{\int_0^\infty dp \int_0^\pi d\theta_p \int_V d^3r' g(\mathbf{r}', p, \theta_p, \lambda)},$$

or, alternatively,  $\theta = [1 + \Pi(\lambda)]/[3 - \Pi(\lambda)]$ .

The respective parts of the radiation which have electric vectors parallel with or perpendicular to the direction of the beam can be expressed by the use of Eqs. (4) and (6) as

$$N_{||}(\Omega_s, \lambda) \Delta\lambda = N_z(\Omega_s, \lambda) \Delta\lambda, \quad (7)$$

$$\begin{aligned} \text{Eq. (7)} &= \frac{2\lambda}{hc} t(\lambda) \Omega_0 \left[ \frac{1 + \Pi(\lambda)}{3 - \Pi(\lambda)} \right] \int_0^\infty dp \int_0^\pi d\theta_p \\ &\times \int_V d^3r' g(\mathbf{r}', p, \theta_p, \lambda) \Delta\lambda + \Delta N_{||} \Delta\lambda, \quad (8) \end{aligned}$$

$$\begin{aligned} N_{\perp}(\Omega_s, \lambda) \Delta\lambda &= N_y(\Omega_s, \lambda) \Delta\lambda + N_x(\Omega_s, \lambda) \Delta\lambda \\ &= \frac{2\lambda}{hc} t(\lambda) \Omega_0 \left[ \frac{1 - \Pi(\lambda)}{3 - \Pi(\lambda)} \right] \int_0^\infty dp \int_0^\pi d\theta_p \\ &\times \int_V d^3r' g(\mathbf{r}', p, \theta_p, \lambda) \Delta\lambda + \Delta N_{\perp} \Delta\lambda. \quad (9) \end{aligned}$$

In Eqs. (8) and (9),  $\Omega_0 \equiv A_{\text{slit}} D^{-2}$ , where  $A_{\text{slit}}$  is the area of the entrance slit, whereas  $\Delta N_{||}$  and  $\Delta N_{\perp}$  are small correction terms which are derived in Appendix I.

If the incremental solid angle in Eq. (1) is integrated over a  $4\pi$ -sr solid angle surrounding  $V$  instead of

merely over the solid angle which the entrance slit subtends on  $V$ , it is found that the total rate at which photons of wavelength  $\lambda$  are emitted from  $V$  in all directions is

$$\begin{aligned} N(\Omega_{4\pi}, \lambda) \Delta\lambda &= \frac{16\pi}{3} \int_0^\infty dp \int_0^\pi d\theta_p \\ &\times \int_V d^3r' g(\mathbf{r}', p, \theta_p, \lambda) (\lambda/hc) \Delta\lambda. \quad (10) \end{aligned}$$

A comparison of Eq. (10) with the sum of Eqs. (8) and (9) gives

$$\begin{aligned} N(\Omega_{4\pi}, \lambda) \Delta\lambda &= \frac{4\pi}{3} \frac{1}{\Omega_0} \left[ \frac{3 - \Pi(\lambda)}{t(\lambda)} \right] \\ &\times [N_{||}(\Omega_s, \lambda) + N_{\perp}(\Omega_s, \lambda) - \Delta N_{||} - \Delta N_{\perp}] \Delta\lambda. \quad (11) \end{aligned}$$

In Eq. (11), the radiation emitted into the total solid angle about  $V$  is expressed in terms of the radiation accepted by the monochromator at the fixed viewing angle of the present geometry. It now remains to find the response of the optical system to  $N_{||, \perp}(\Omega_s, \lambda) \Delta\lambda$  and to extend Eq. (11) to the case of emission into a finite spectral interval.

## The Response to a Spectral Feature

The rate at which photons from  $V$  having wavelengths in an isolated spectral feature  $\zeta$  are admitted by the entrance slit of the monochromator is given by

$$W(\Omega_s) = W_{||}(\Omega_s) + W_{\perp}(\Omega_s), \quad (12)$$

where

$$W_{||, \perp}(\Omega_s) = \int_0^\infty \Phi_{\zeta}(\lambda) N_{||, \perp}(\Omega_s, \lambda) d\lambda,$$

while  $\Phi_{\zeta}(\lambda) = 1$  if  $\lambda$  is within the wavelength interval of  $\zeta$ , otherwise  $\Phi_{\zeta}(\lambda) = 0$ .

To relate  $W(\Omega_s)$  to the total integrated response of the optical system as it scans through  $\zeta$ , it is necessary to take into account the responsivity of the optical system as a function of the polarization of the incident light. The development here will be carried out only for radiation having electric vectors parallel with the beam; however, the development for the perpendicularly polarized radiation proceeds in the same manner.

Let  $S_{||}(\lambda, \Lambda)$  be defined as the response of the optical system to a monochromatic input  $\delta(\lambda' - \lambda)$  which has electric vectors parallel with the beam. For a polychromatic input  $\Phi_{\zeta}(\lambda) N_{||}(\Omega_s, \lambda) \Delta\lambda$ , the response at a setting  $\Lambda$  is given by

$$\int_0^\infty \Phi_{\zeta}(\lambda) S_{||}(\lambda, \Lambda) N_{||}(\Omega_s, \lambda) d\lambda. \quad (13)$$

The total integrated response over all settings is

$$\begin{aligned} J_{||} &= \int_0^\infty d\lambda \int_0^\infty d\Lambda \Phi_{\zeta}(\lambda) N_{||}(\Omega_s, \lambda) S_{||}(\lambda, \Lambda) \\ &= \int_0^\infty I_{||}(\lambda) \Phi_{\zeta}(\lambda) N_{||}(\Omega_s, \lambda) d\lambda, \quad (14) \end{aligned}$$

where

$$I_{11}(\lambda) = \int_0^{\infty} S_{11}(\lambda, \Delta) d\Delta.$$

It has been previously shown<sup>12</sup> that

$$W_{11} = [J_{11}/I_{11}(\lambda_0)] - [\Delta J_{11}/I_{11}(\lambda_0)]. \quad (15)$$

This relationship is a consequence of the usually slow variation of  $I_{11}(\lambda)$  with  $\lambda$  over the wavelength region in which  $\Phi_{\zeta}(\lambda)N_{11}(\Omega_s, \lambda)$  is appreciable. Thus, one can write

$$I_{11}(\lambda) = I_{11}(\lambda_0) + \Delta I_{11}(\lambda), \quad (16)$$

where  $\lambda_0$  is a central wavelength in  $\zeta$  and  $\Delta I_{11}(\lambda) = I_{11}(\lambda) - I_{11}(\lambda_0)$  is a small quantity. Also in Eq. (15),

$$\Delta J_{11} = \int_0^{\infty} \Phi_{\zeta}(\lambda) N_{11}(\Omega_s, \lambda) \Delta I_{11}(\lambda) d\lambda. \quad (17)$$

From the expression for  $W_{11}(\Omega_s)$  in Eq. (15) and the analogous expression for  $W_{\perp}(\Omega_s)$ , the total irradiance of the slit is given by

$$W(\Omega_s) = \frac{J_{11}}{I_{11}(\lambda_0)} + \frac{J_{\perp}}{I_{\perp}(\lambda_0)} - \frac{\Delta J_{11}}{I_{11}(\lambda_0)} - \frac{\Delta J_{\perp}}{I_{\perp}(\lambda_0)}. \quad (18)$$

The total rate at which photons with wavelengths in  $\zeta$  are emitted in all directions with all polarizations is obtained by integrating Eq. (11) over all wavelengths. The integral to be evaluated is

$$\begin{aligned} W(\Omega_{4\pi}) &= \int_0^{\infty} N(\Omega_{4\pi}, \lambda) d\lambda \\ &= \frac{4\pi}{3} \frac{1}{\Omega_0} \int_0^{\infty} \Phi_{\zeta}(\lambda) \frac{[3 - \Pi(\lambda)]}{t(\lambda)} \\ &\times [N_{11}(\Omega_s, \lambda) + N_{\perp}(\Omega_s, \lambda) - \Delta N_{11} - \Delta N_{\perp}] d\lambda. \quad (19) \end{aligned}$$

If  $t(\lambda)$  is constant over wavelengths in  $\zeta$  and if an average polarization is defined by

$$\begin{aligned} \Pi(\zeta) &\equiv \\ &\frac{\int \Phi_{\zeta}(\lambda) \Pi(\lambda) [N_{11}(\Omega_s, \lambda) + N_{\perp}(\Omega_s, \lambda) - \Delta N_{11} - \Delta N_{\perp}] d\lambda}{\int \Phi_{\zeta}(\lambda) [N_{11}(\Omega_s, \lambda) + N_{\perp}(\Omega_s, \lambda) - \Delta N_{11} - \Delta N_{\perp}] d\lambda}, \quad (20) \end{aligned}$$

then Eq. (19), with the aid of Eqs. (12) and (18), can be expressed as

$$\begin{aligned} W(\Omega_{4\pi}) &= \frac{4}{3} \frac{1}{\Omega_0} \left[ \frac{3 - \Pi(\zeta)}{t(\zeta)} \right] \\ &\times \left[ \frac{J_{11}}{I_{11}(\lambda_0)} + \frac{J_{\perp}}{I_{\perp}(\lambda_0)} - \frac{\Delta J_{11}}{I_{11}(\lambda_0)} - \frac{\Delta J_{\perp}}{I_{\perp}(\lambda_0)} - \Delta W(\Omega_{4\pi}) \right], \quad (21) \end{aligned}$$

where

$$\Delta W(\Omega_{4\pi}) \equiv \int_0^{\infty} \Phi_{\zeta}(\lambda) [\Delta N_{11} + \Delta N_{\perp}] d\lambda.$$

The final expression for  $\Delta W(\Omega_{4\pi})$  will be obtained from Eq. (21) by expressing  $I_{11}(\lambda_0)$  and  $I_{\perp}(\lambda_0)$  in terms of the response of the optical system to the blackbody standard.

### Comparison with a Blackbody Standard

Blackbody radiation from an isothermal cavity at a temperature  $T$  can be described by Planck's function  $B(\lambda, T)$ , which denotes the amount of power radiated in a wavelength interval between  $\lambda$  and  $\lambda + \Delta\lambda$  which is emitted per unit solid angle normal to the blackbody aperture. In the following, it is assumed that  $B(\lambda, T)$  has no spatial dependence over the aperture, that the emissivity of the blackbody is unity, that the radiation is unpolarized, and that the emission in a direction  $\theta_b$  measured from the central normal to the aperture of the blackbody is given by  $B(\lambda, T) \cos\theta_b$ . All of these assumptions are well met for the blackbody and the geometry used in this laboratory (maximum  $\theta_b$  is less than  $3^\circ$ ).

The rate at which photons of wavelength  $\lambda$  from the blackbody aperture are intercepted by the slit is

$$\begin{aligned} \Gamma(\Omega_s, \lambda) \Delta\lambda &= \frac{t(\lambda) \lambda \Delta\lambda}{hc} B(\lambda, T) \int_{A_{ap}} dA \int_{A_{slit}} \cos\theta_b d\omega \\ &= t(\lambda) \frac{\lambda \Delta\lambda}{hc} B(\lambda, T) (A_{slit}/R^2) A_{ap} (1 - \delta_b), \quad (22) \end{aligned}$$

where  $\Delta\omega$  is the solid angle which an incremental slit area subtends at an incremental aperture area  $\Delta A$  of the aperture area  $A_{ap}$ . The quantity  $\delta_b$  is a small correction factor given by

$$\delta_b = \frac{A_{ap}}{\pi R^2} + \frac{(a^2 + b^2)}{6R^2} + \dots \quad (23)$$

Let  $\Gamma_{11}(\Omega_s, \lambda)$  and  $\Gamma_{\perp}(\Omega_s, \lambda)$  be the components, respectively, of  $\Gamma(\Omega_s, \lambda)$  whose electric vectors are parallel with or perpendicular to the direction of the beam. Since the radiation is nonpolarized,

$$\Gamma_{11}(\Omega_s, \lambda) = \Gamma_{\perp}(\Omega_s, \lambda) = [\Gamma(\Omega_s, \lambda)/2]. \quad (24)$$

The response of the optical system at a setting  $\Lambda_0$  to an input  $\Gamma(\Omega_s, \lambda)$  is given by

$$\begin{aligned} H(\Lambda_0) &= \int_0^{\infty} \Gamma_{11}(\Omega_s, \lambda) S_{11}(\lambda, \Lambda_0) d\lambda \\ &\quad + \int_0^{\infty} \Gamma_{\perp}(\Omega_s, \lambda) S_{\perp}(\lambda, \Lambda_0) d\lambda \\ &= \Gamma_{11}(\Omega_s, \lambda_0) \int_0^{\infty} S_{11}(\lambda, \Lambda_0) d\lambda \\ &\quad + \Gamma_{\perp}(\Omega_s, \lambda_0) \int_0^{\infty} S_{\perp}(\lambda, \Lambda_0) d\lambda + \Delta H(\Lambda_0), \quad (25) \end{aligned}$$

where

$$\Delta H(\Lambda_0) = \int_0^{\infty} \Delta \Gamma_{11} S_{11}(\lambda, \Lambda_0) d\lambda + \int_0^{\infty} \Delta \Gamma_{\perp} S_{\perp}(\lambda, \Lambda_0) d\lambda,$$

and

$$\Delta\Gamma_{||} = \Gamma_{||}(\Omega_s, \lambda) - \Gamma_{||}(\Omega_s, \lambda_0),$$

$$\Delta\Gamma_{\perp} = \Gamma_{\perp}(\Omega_s, \lambda) - \Gamma_{\perp}(\Omega_s, \lambda_0).$$

Also, let

$$\int_0^{\infty} S_{\perp}(\lambda, \Lambda_0) d\lambda = \alpha \int_0^{\infty} S_{||}(\lambda, \Lambda_0) d\lambda, \quad (26)$$

and

$$J_{\perp} = \beta J_{||}. \quad (27)$$

The total integrated response of the system to the spectral feature  $\zeta$  can now be expressed as

$$J_{\zeta} = J_{||} + J_{\perp} = (1 + \beta) J_{||}, \quad (28)$$

and the response of the system to  $\Gamma(\Omega_s, \lambda)$  becomes

$$H(\Lambda_0) = \Gamma(\Omega_s, \lambda_0) (1 + \alpha) \int_0^{\infty} S_{||}(\lambda, \Lambda_0) d\lambda + \Delta H(\Lambda_0). \quad (29)$$

If the result for  $W(\Omega_{4\pi})$  in Eq. (21) is now recalled, and if

$$\int_0^{\infty} S_{||}(\lambda, \Lambda_0) d\lambda$$

is expressed in terms of  $H(\Lambda_0)$  by the use of Eq. (29), the desired result is obtained as

$$W(\Omega_{4\pi}) = \frac{4\pi D^2 \lambda B(\lambda_0, T) A_{ap} J_{\zeta}}{hc R^2 H(\Lambda_0)} \chi(\zeta) [1 + \Sigma], \quad (30)$$

where

$$\chi(\zeta) \equiv \frac{3 - \Pi(\zeta) (\alpha + \beta) (1 + \alpha)}{3 - 2\alpha (1 + \beta)}.$$

The correction term  $\Sigma$ , expanded to first order, is

$$\Sigma = \frac{\Delta H}{H} - \delta_b + \frac{\alpha}{\alpha + \beta} \times \left( \Delta S_{||} + \frac{\beta}{\alpha} \Delta S_{\perp} - \frac{\Delta J_{||}}{J_{||}} - \frac{\Delta W(\Omega_{4\pi})}{W_{||}(\Omega_s)} - \frac{\beta}{\alpha} \frac{\Delta J_{\perp}}{J_{\perp}} \right), \quad (31)$$

where

$$\Delta S_{||} \equiv \left( \int_0^{\infty} S_{||}(\lambda, \Lambda_0) d\lambda \right) / \left( \int_0^{\infty} S_{||}(\lambda_0, \Lambda) d\Lambda \right) - 1,$$

$$\Delta S_{\perp} \equiv \left( \int_0^{\infty} S_{\perp}(\lambda, \Lambda_0) d\lambda \right) / \left( \int_0^{\infty} S_{\perp}(\lambda_0, \Lambda) d\Lambda \right) - 1.$$

To complete the procedure for obtaining emission cross sections, the relationship of  $W(\Omega_{4\pi})$  to the emission cross section  $\sigma_{\zeta}$  is

$$\sigma_{\zeta} \equiv W(\Omega_{4\pi}) / i_0 \eta l, \quad (32)$$

where  $i_0$  is the rate at which beam particles are incident on the target gas and  $\eta$  is the number density of the gas. The relationship is, in general, valid only if the emission properties over the observed length  $l$  of the beam do not vary appreciably.

## The Correction Term

From Eq. (31), the correction term  $\Sigma$  can be seen to arise from five sources of error: (1) the geometries used in making the optical measurements of the beam and of the calibration source (as represented in  $\delta_b$  and  $\Delta W(\Omega_{4\pi})/W_{||}(\Omega_s)$ ), (2) the responsivity of the optical system as a function of wavelength ( $\Delta S_{||,\perp}$  and  $\Delta J_{||,\perp}/J_{||,\perp}$ ), (3) the responsivity of the optical system as a function of the polarization of the incident light ( $\alpha$  and  $\beta$ ), (4) the variation of the spectral radiance of the calibration source over the bandwidth of a spectral feature ( $\Delta H/H$ ), and (5) the angular distribution of the radiation from the beam ( $\beta$ ).

To set bounds on  $\Sigma$ , one must consider the geometry of the specific monochromator used, in concert with the spectral width and central wavelength of each emission feature. As an example,  $\Sigma$  will be evaluated for the (0, 0)  $N_2^+$  first negative band under single collision conditions for excitation by proton and electron impact. The monochromator used in this example is an Ebert 0.5-m instrument which has been discussed in a previous paper.<sup>12</sup> The spectral feature of this example lies within a 30-Å band centered at roughly 3900 Å.

Some of the terms appearing in  $\Sigma$  have been previously evaluated.<sup>12</sup> Estimates for these quantities include

$$|\Delta S_{||}| \simeq |\Delta S_{\perp}| \leq 0.01,$$

$$|\Delta J_{||}/J_{||}| \simeq |\Delta J_{\perp}/J_{\perp}| \leq 0.01,$$

$$|\Delta H/H| \leq 0.022 \text{ for } T = 1271 \text{ K.}$$

The value of  $\alpha$  at  $\lambda_0$  is found from the polarization fraction measured when nonpolarized light is sent through the monochromator. For the present case,  $\alpha$  is about 0.97. For excitation by proton and electron impact, a representative value<sup>2,9</sup> of the average polarization fraction of the (0,0) band is 5%. The measured value of the polarization fraction  $\Pi_0$  is obtained from the formula:

$$\Pi(\lambda) \simeq (\Pi_0 - \Pi_g) / (1 + \Pi_0 \Pi_g), \quad (33)$$

where

$$\Pi_g \simeq (1 - \alpha) / (1 + \alpha) \quad \text{and} \quad \beta \simeq (1 - \Pi_0) / (1 + \Pi_0).$$

These values of  $\alpha$  and  $\Pi(\zeta)$  yield a value of 0.94 for  $\beta$ . The value of  $\delta_b$  is less than 0.005 for the geometry of Table I.

Upper and lower bounds on  $\Delta W(\Omega_{4\pi})/W_{||}(\Omega_s)$  can be obtained by the use of the expressions for  $\Delta N_{||}$  and  $\Delta N_{\perp}$  given in Eq. (38) of Appendix I, along with the aid of the theorem on integrals given as Eq. (33) of Ref. 12. The result is  $|\Delta W(\Omega_{4\pi})/W_{||}(\Omega_s)| \leq 0.025$ .

## Conclusions

In the example presented, the dominant contribution to the correction term  $\Sigma$  arises from geometrical considerations of extended radiation sources. Smaller contributions to  $\Sigma$  are made by variations in the responsivity of the optical system and in the spectral radiance of the calibration source over the bandwidth of the spectral feature. For this example, uncertainties

arising from the angular distribution of radiation and the variation in the responsivity of the optical system as a function of the polarization of incident light are negligible.

Summation of the terms contributing to  $\Sigma$  indicates that  $|\Sigma| \leq 0.05$  for the (0, 0)  $N_2^+$  first negative band. This value is considerably smaller than the combined accuracy ( $\pm 20\%$ ) of emission cross section measurements for this band. Calculations of  $\Sigma$  for other emission features of bandwidth less than 40 Å in the spectral range 3800–6000 Å show that  $|\Sigma| < 0.1$ . Thus, it is concluded that, for this geometry, the neglect of  $\Sigma$  in Eq. (30) introduces a small but significant uncertainty in the emission cross sections for such spectral features.

We note that this technique is especially suited for polarization and cross section measurements in which  $\Sigma$  and  $\delta\Pi_e$  are desired to be minimal. This reduction is accomplished primarily by the use of large source-detector separations. In addition, considerable simplicity is attained by the absence of lenses or other light gathering aids between the source and monochromator entrance slit. The absence of a lens does, of course, limit optical measurements to the more intense spectral features.

The technique can be extended to weaker emission features by appropriately normalizing the relative cross section data obtained with the aid of a lens system to the absolute cross section data obtained by the present method. It is important that any changes in the emission as a function of position along the beam be accounted for in the normalization process. In this procedure some increase in  $\Sigma$ , depending on spectral feature and geometry, is to be expected.

As evident from Eq. (32), emission cross section data for which bounds on  $\Sigma$  have not been placed are subject to significant systematic error. Consequently, it is cautioned that any scheme to increase the energy accepted by the optical system, such as by modification of the geometry or other factors, should be tempered with a knowledge of  $\Sigma$  for each particular spectral feature and geometry under consideration.

The research reported in this paper was sponsored by the Air Force Cambridge Research Laboratories, Office of Aerospace Research, but the report does not necessarily reflect endorsement by the sponsor.

## Appendix I

In this section, expressions for the quantities  $\Delta N_{||}$  and  $\Delta N_{\perp}$ , which appear in Eqs. (8) and (9), are derived.

Let us define the operators  $F_1$  and  $F_2$  which act on a quantity  $\xi(r', p, \theta_p, \lambda)$  in the following manner:

$$F_1[\xi] = \int_0^\infty dp \int_0^\pi d\theta_p \int_V d^3r' \xi g(r', p, \theta_p, \lambda), \quad (\text{A-1})$$

$$F_2[\xi] = \int_0^\infty dp \int_0^\pi d\theta_p \int_V d^3r' \xi g(r', p, \theta_p, \lambda) \cos^2\theta_p. \quad (\text{A-2})$$

By use of these operators and the result in Eq. (4), expressions for  $N_m(\Omega_s, \lambda)$  with  $\hat{m} = \hat{x}, \hat{y}$ , and  $\hat{z}$  can be given as

$$\begin{aligned} N_x(\Omega_s, \lambda) \Delta\lambda &= [\lambda t(\lambda)/hc] \Omega_0 \{F_1[\delta_x] + F_2[\delta_x']\} \Delta\lambda, \\ N_y(\Omega_s, \lambda) \Delta\lambda &= [\lambda t(\lambda)/hc] \\ &\times \Omega_0 \{F_1[1 + \delta_y] - F_2[1 + \delta_y]\} \Delta\lambda, \quad (\text{A-3}) \end{aligned}$$

$$N_z(\Omega_s, \lambda) \Delta\lambda = [\lambda t(\lambda)/hc] \Omega_0 \{F_1[\delta_z] + F_2[2 + \delta_z']\} \Delta\lambda.$$

The expressions for the  $\delta$  quantities, correct to order  $D^{-2}$ , are

$$\begin{aligned} \delta_x &= (b^2/12D^2) + (y'^2/D^2), \\ \delta_x' &= [(2a^2 - b^2)/12D^2] + (2z'^2 - y'^2)/D^2, \quad (\text{A-4}) \\ \delta_y &= \frac{2x'}{D} + \frac{6x'^2 - 5y'^2 - 3z'^2}{2D^2} - \frac{5b^2 + 3a^2}{24D^2}, \\ \delta_z &= (a^2/12D^2) + (z'^2/D^2), \\ \delta_z' &= \frac{4x'}{D} + \frac{6x'^2 - 3y'^2 - 8z'^2}{D^2} - \frac{8a^2 + 3b^2}{12D^2}. \end{aligned}$$

For the geometry of Table I the  $\delta$  quantities are much smaller than unity. Separation of these incremental quantities from those of order unity leads to the designation of  $\Delta N_{||}$  and  $\Delta N_{\perp}$ , respectively, as

$$\begin{aligned} \Delta N_{||} \Delta\lambda &= [\lambda t(\lambda)/hc] \Omega_0 \{F_1[\delta_z] + F_2[\delta_z']\} \Delta\lambda, \\ N_{\perp} \Delta\lambda &= [\lambda t(\lambda)/hc] \Omega_0 \{F_1[\delta_x + \delta_y] \\ &+ F_2[\delta_x' - \delta_y']\} \Delta\lambda. \quad (\text{A-5}) \end{aligned}$$

## Appendix II

To set bounds on  $\delta\Pi_e(\lambda)$ , the definition of the polarization fraction given in Eq. (5) is compared with the experimentally measured polarization fraction given by

$$\Pi_e(\lambda) = \frac{N_{||}(\Omega_s, \lambda) \Delta\lambda - N_{\perp}(\Omega_s, \lambda) \Delta\lambda}{N_{||}(\Omega_s, \lambda) \Delta\lambda + N_{\perp}(\Omega_s, \lambda) \Delta\lambda}. \quad (\text{B-1})$$

Since the monochromator slit is perpendicular to the beam direction,

$$N_{||}(\Omega_s, \lambda) \Delta\lambda = N_z(\Omega_s, \lambda) \Delta\lambda, \quad (\text{B-2})$$

$$N_{\perp}(\Omega_s, \lambda) \Delta\lambda = N_x(\Omega_s, \lambda) \Delta\lambda + N_y(\Omega_s, \lambda) \Delta\lambda.$$

If the appropriate expressions for  $N_m(\Omega_s, \lambda) \Delta\lambda$  given in Appendix I are substituted into Eq. (40), one finds that

$$\begin{aligned} \Pi_e(\lambda) &= \\ &= \frac{-1 + 3\theta + \{F_1[\delta_z - \delta_x - \delta_y] + F_2[\delta_z' - \delta_x' + \delta_y']\} (F_1[1])^{-1}}{1 + \theta + \{F_1[\delta_z + \delta_x + \delta_y] + F_2[\delta_z' + \delta_x' - \delta_y']\} (F_1[1])^{-1}}, \quad (\text{B-3}) \end{aligned}$$

where  $F_2[1]/F_1[1] = \theta$ . If  $\theta$  is greater than zero, the expression for  $\Pi_e(\lambda)$  may be expanded as

$$\Pi_e(\lambda) = \Pi(\lambda) + \delta\Pi_e(\lambda), \quad (\text{B-4})$$

with

$$\begin{aligned} & \delta\Pi_e(\lambda) \\ &= \frac{3 - \Pi(\lambda)}{4F_1[1]} \{F_1[\delta_z - \delta_x - \delta_y] + F_2[\delta_z' - \delta_x' + \delta_y']\} \\ & \quad - \frac{\Pi(\lambda)[3 - \Pi(\lambda)]}{4F_1[1]} \{F_1[\delta_z + \delta_x + \delta_y] \\ & \quad + F_2[\delta_z' + \delta_x' - \delta_y']\}. \quad (\text{B-5}) \end{aligned}$$

In the limit as  $D$  becomes infinite,  $\delta\Pi_e(\lambda)$  is zero and  $\Pi_e(\lambda)$  reduces to  $\Pi(\lambda)$ .

## References

1. J. L. Philpot and R. H. Hughes, Phys. Rev. **133**, A107 (1964).
2. J. W. McConkey, J. M. Woolsey, and D. J. Burns, Planet. Space Sci. **15**, 1332 (1967).

3. J. W. McConkey and I. D. Latimer, Proc. Phys. Soc. **86**, 463 (1965).
4. R. F. Holland, Los Alamos Scientific Laboratory, Rep. LA-3783.
5. B. N. Srivastava and I. M. Mirza, Phys. Rev. **168**, 86 (1968).
6. S. Hayakawa and H. Nishimura, J. Geomag. Geoelec. **16**, 72 (1964).
7. D. T. Stewart, Proc. Phys. Soc. **A69**, 437 (1956).
8. J. M. Robinson and H. B. Gilbody, Proc. Phys. Soc. **92**, 589 (1967).
9. M. Dufay, J. Desequelles, M. Druetta, and M. Eidelsberg, Ann. Geophys. **22**, 614 (1966).
10. E. W. Thomas, G. D. Bent, and J. L. Edwards, Phys. Rev. **165**, 32 (1968).
11. W. F. Sheridan, O. Oldenberg, and N. P. Carleton, *Abstracts of Second International Conference on the Physics of Electronic and Atomic Collisions*, University of Colorado (W. A. Benjamin, Inc., New York, 1961), p. 159.
12. J. J. Merrill and R. G. Layton, Appl. Opt. **5**, 1818 (1966)

## INTER-SOCIETY COLOR COUNCIL

## COLOUR GROUP

### JOINT MEETING, 16-17 June 1969 London

A Joint Meeting of the Inter-Society Color Council and the Colour Group (Great Britain) will be held at Imperial College, London on 17 June, preceded by a social event on 16 June. This will be the first international meeting of these societies; it is scheduled to follow the AIC Color 69 Stockholm Meeting in the hope that many of the U. S. participants in the latter can arrange to stay over for the London meeting. Dorothy Morley of the Colour Group has arranged a program of informal discussions by British participants: **Keith McLaren**, ICI (amplification of his Stockholm paper on computer match prediction and color differences), **Jean Noir**, Courtaulds (color difference formulas), **A. E. Cutler** (new computer for match prediction), **David Palmer** Institute of Ophthalmology (amplification of his Stockholm paper on the varying weighting of luminance with intensity), and **C. A. Padgham**, City University (psychophysical techniques for luminosity scaling). There will also be U. S. contributions to the London program, but at the time of going to press no details are available. For further information write Fred W. Billmeyer, Jr., Chemistry Department, Rensselaer Polytechnic Institute, Troy, N. Y. 12181.

## OSA Technical Groups

### Atmospheric Optics 10 October 1968

The Atmospheric Optics Technical Group held a joint meeting on 10 October 1968 with the Atmospheric Optics Specialty Group of the Infrared Information Symposium (IRIS). Scattering by aerosols in the atmosphere was the featured topic for discussion. Approximately eighty people were present.

Franklin S. Harris, Jr., chairman of the IRIS Specialty Group, introduced Kurt Bullrich, a professor at the Meteorological-Geophysical Institute, Johannes-Gutenberg University in Mainz, Germany. Bullrich described some of the remaining problems in scattering and discussed various phases of research being conducted in his laboratory. The problems being considered there include scattering as a function of refractive index, effect of relative humidity on refractive index, multiple scattering, and absorption by aerosol particles. Considerable work is also being done on the albedo of different types of natural terrain. Radiant energy going out into space has been calculated for various wavelengths and solar angles. Sky radiance maps have been generated, by use of a computer, from data obtained by photometric photography of the sky. Some effort has been directed toward measuring the real part of the index of refraction of atmospheric aerosols by an immersion technique, which quantity depends quite strongly on relative humidity. Bullrich concluded by describing a two-ended laser system being set up to probe the upper atmosphere for aerosol layers; experiments will be carried out over a 200-km baseline.

The remainder of the period was spent in informal discussion of Bullrich's talk, of papers presented in a previous OSA meeting

ROBERT J. POTTER  
Chairman, Technical Council

contributed papers session, and of some unpublished experimental results. William Elliott presented results obtained in a balloon-nephelometer experiment in which the light scattered at  $25^\circ$  and  $155^\circ$  by a 15-cm cube of air was measured, and there was considerable discussion of his results. Some satellite data obtained by Douglas Rawcliffe *Aerospace* on the radiance of cloud tops were presented and discussed.

The general problem of radiative transfer in a nonhomogeneous atmosphere was considered, as was the reliability of existing data on the real and imaginary indices of water and ice which are used in Mie theory calculations. The consensus was that these quantities are known sufficiently well, except over a few narrow spectral intervals, from the visible to more than  $20 \mu$ .

## Errata

**F. Grum and G. W. Luckey**, Optical Sphere Paint and a Working Standard of Reflectance, Appl. Opt. **7**, 2289 (1968):

p. 2290, right-hand column, footnote should read: "The powder may be obtained from Distillation Products Industries, under the name Eastman White Reflectance Standard." The footnote printed on p. 2290 refers to the "white optical paint" mentioned in line 7.

p. 2292, Fig. 6 caption should be changed as follows: (0) Eastman White Reflectance paint; (4) should be deleted; (5) should be renumbered as (4).

p. 2293, Fig. 11 caption should read: (2) sphere coated with Eastman White Reflectance paint.

p. 2293, left-hand column, line 5 of the Discussion should read: "adverse environmental conditions. Smoked magnesium oxide."